Chapter 8: Scour hole

8.1. Introduction

Unsteady flows in river are sometimes associated with a rapid change in solid discharge. A solid discharge fluctuation can be the result of a variation in the shear stress applied to the bed, as it is the case in transcritical flows. Another reason can be a change in the bed properties, modifying the shear stress resisting to the flow. For example, it occurs in the case of a transition between a non-erodible bed and an erodible one. At the transition, the solid discharge increases. According to common solid transport formulae, this rise is considered to be sharp and instantaneous, the discharge changes from zero to its equilibrium value. But actually, the solid discharge needs time and space to reach its equilibrium value (Fig. 8.1).

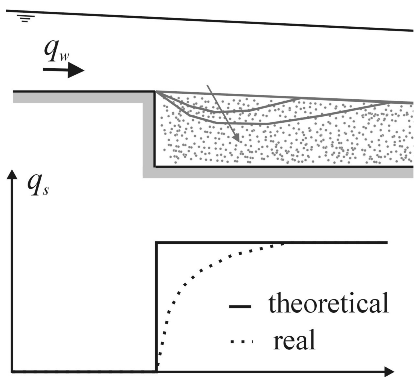

Figure 8.1. Transition between a fixed bed: spatial lag in solid discharge

Under such unsteady conditions, the classical formulae based on equilibrium states are not fully satisfactory. In order to improve the calculation of the solid discharge in such unsteady conditions, Bell and Sutherland (1983), Philips and Sutherland (1989) (for example) proposed spatial and temporal lags. As the two-layer approach is not developed under equilibrium conditions, there is a hope that the creation process of the sediment transport layer could replace such lags. Two cases were reproduced experimentally and numerically: (1) the transition between a fixed and an erodible bed under a subcritical flow and (2) an erodible bed at the toe of a fixed sill, under transcritical conditions. In both cases the evolution of the scour hole at the transition is studied.

8.2. Transition between a fixed and a mobile bed

8.2.1. Experiment

Within the framework of this thesis, a series of experiment to investigate the sediment transport under non-equilibrium conditions were performed. These experiments were carried out in the Civil Engineering Laboratory of the Université catholique de Louvain in collaboration with M. Iervolino (Iervolino, 2005) from the Università degli Studi di Napoli "Frederico II". The formation of a scour hole due to the transition from a fixed to an erodible bed is investigated under subcritical flow rates. Previously, similar experiments were realised by Bell and Sutherland (1983) and Philips and Sutherland (1989) in order to propose spatial and temporal lags to improve the solid discharge calculation under unsteady flow conditions. The experimental set-up is the one described in chapter 5, a non-erodible structure is positioned in the upstream part of the flume. The 2-m long fixed structure is followed downstream by a sand bed (Fig. 8.2). Grains of sand are glued on the fixed structure in order to have the same bed roughness along the whole flume. A floating panel is placed at the entrance of the flume to smooth the free surface.

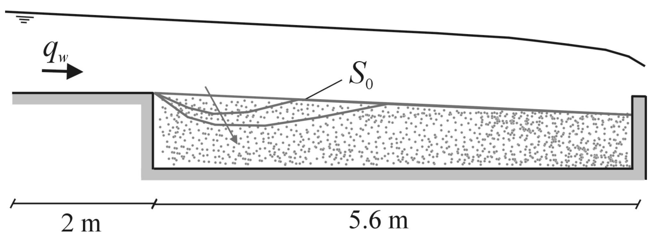

Figure 8.2. Transition between a fixed bed: experimental configuration

The water level, controlled at the downstream end, is measured with an ultrasonic probe, while the bed level is measured with a bed profiler. Both levels are measured at a rate of 25 measurements per second at every 5 cm, the distance from the upstream end is measured with a potentiometer. These devices were assembled on a trolley moving on rails placed above the side walls of the flume. In addition, a digital camera is positioned at the bed transition to follow the evolution of the scour hole with time. Every 2 minutes, one picture is taken, capturing a 90 cm-large window. The interface between water and sediments is deduced from digital imaging treatment. Figure 8.3 is an example of a picture taken by the digital camera. The white lines define the fixed bed.

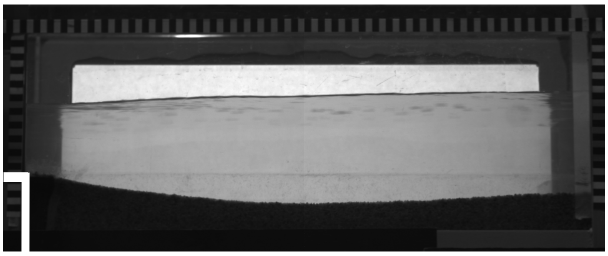

Figure 8.3. Example of an image taken with the digital imaging
(1 graduation = 1 cm)

The configuration and the position of the camera ensure a precision better than one millimetre. More details about these experimental devices are exposed in chapter 5 section 5.7.

At the beginning of the experiment, the downstream end of the flume is obstructed, a small water discharge is provided in order to saturate the sand and to increase the water level without disturbing the initial flat erodible bed. When the water level reaches the uniform water depth, the downstream obstruction is removed and the discharge is increased until it reaches the value of the experimental run. A short time is necessary to obtain the experimental conditions.

A range of water discharges was tested (Table 8.1). The sand is uniform with a median diameter of 1.65 mm, its grain-size distribution is shown in section 5.4.1 of chapter 5. The flow is not supplied with sediment upstream. All the experimental runs correspond to subcritical flows. The fixed bottom is horizontal and the initial slope of the erodible bed is variable (on an average of 0.3%). The water level is imposed by a downstream weir, which is 2 cm above the downstream bed level.

Run #	S_0 (%)	Q_w (l/s)	Duration
1	0.11	25	7h17
2	0.36	30	2h20
3	0.29	36	1h34
4	0.35	33	8h46
5	0.30	38	6h05
6	0.26	38	6h10
7	0.38	38.5	7h37
8	0.34	28.7	7h31

Table 8.1. Experimental data

Preliminary tests revealed a lateral asymmetry of the scour hole due to the asymmetric geometry of the upstream tank, which leads to a lateral component of velocity at the entrance of the flume. The tank geometry was improved to correct the direction of the flow at the entrance. The bed and water levels are measured with the probes at the centre of the flume. They give the average levels in a cross section. At the same time, the levels from the video camera are taken at a side wall of the flume.

8.2.2. Experimental results

8.2.2.1. Bed level evolution

The time-evolution of the bed profile is plotted for different times in Figure 8.4 for run 7 (Table 8.1). The level of the bed is set to zero at the transition from non-erodible to erodible bed, which is located 2 m downstream from the entrance of the flume. The location of the maximum scour does not change significantly with time. At the beginning of the experiment, there is a deposition at the end of the scour hole. A short time after the beginning of the experiment (≈ 30 min for run 7), the scour hole has already developed all along the flume. Then, there is a general erosion and sediments are evacuated over the weir at the downstream end.

As observed by Phillips and Sutherland (1992), dunes propagate downstream. At the beginning of the experiment, the height of the dunes is quite important in comparison with the dimensions of the scour hole. Contrary to the scour hole, which deepens with time, the dune dimension remains at the same order of magnitude during the entire duration of the experiment.

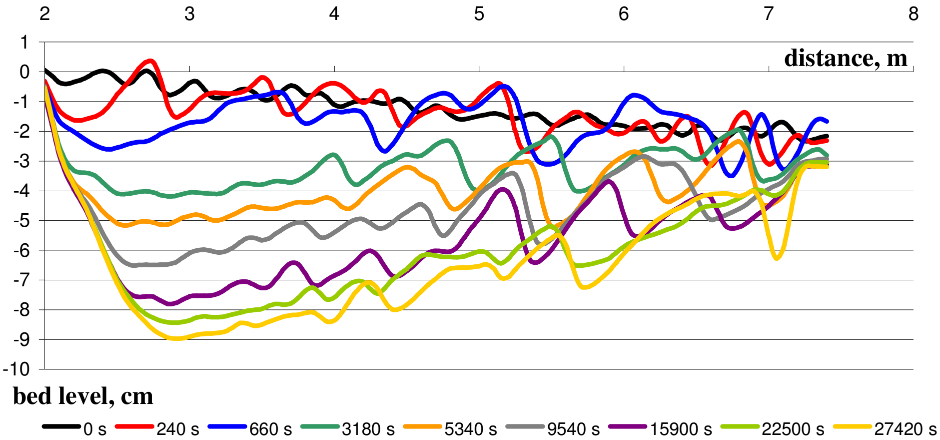

Figure 8.4. Bed level evolution (run 7)

The bed profiles are represented in a non-dimensional way in Figure 8.5. The *x*-coordinate corresponds to the distance from the transition divided by the maximum scour depth and the *y*-coordinate is the scour depth divided by the maximum scour depth. The bed profile is auto-similar in time, meaning the shape of the scour hole remains approximately the same with time. To plot Figure 8.5, the abscissa are limited to the length of the scour hole, which corresponds to the whole flume at the end of the experiment. At the early stages of the experiment, the bed forms affect the shape of the scour hole and the similarity is slightly poorer (t = 240 s). At the end of the experiment, bed-forms are present in the downstream part of the scour hole. This implies that the similarity is less precise there.

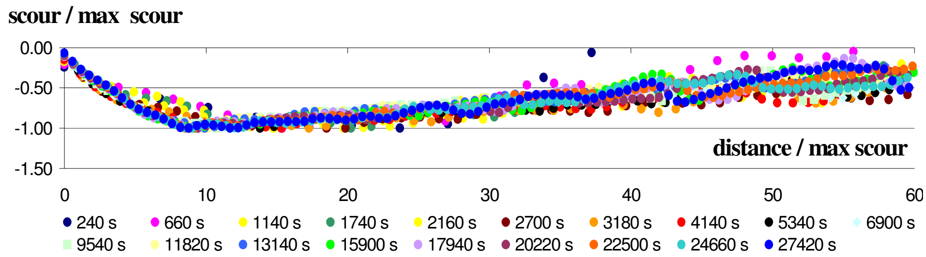

Figure 8.5. Non-dimensional bed level evolution (run 7)

The non-dimensional profile can be interpolated by a curve:

$$\frac{(z_b - z_0)}{(z_b - z_0)_{\max}} = f\left(\frac{x}{(z_b - z_0)_{\max}}\right) \tag{8.1}$$

where z_b is the bed level, z_0 is the initial bed level and x is the distance from the bed transition. Iervolino (2005) used an expression proposed by Erto (1999) depending on three non-dimensional parameters (α, β, L):

$$\frac{(z_b - z_0)}{(z_b - z_0)_{\max}} = -\frac{\beta}{\alpha}\left(\frac{1}{\alpha L}\frac{x}{(z_b - z_0)_{\max}}\right)^{\beta-1} e^{-\left(\frac{1}{\alpha L}\frac{x}{(z_b - z_0)_{\max}}\right)^{\beta}} \tag{8.2}$$

For each experiment (Table 8.1), identically to Figure 8.5 for run 7, an auto-similar profile of the scour hole can be plotted. The auto-similar profiles are not identical from an experiment to another, but all can be interpolated with the formula (8.2). Iervolino (2005) calculated the three coefficients for all the experimental runs. For all the runs, the coefficients $\alpha \approx 2.15$ and $\beta \approx 0.333$ are quite steady, but the coefficient L is varying a lot, implying no general formulation can be deduced.

8.2.2.2. Maximum scour depth

In practical problems, it is interesting to predict the time-evolution of the maximum scour depth. In literature, several authors worked on this topic. Gaudio et al. (2000) predicted the equilibrium dimensions of the scour hole (equilibrium length and maximum depth) based on the results of experiments on a bed consisting of a succession of sills (after each sill a scour hole developed). In this experimental work, the equilibrium length of the scour hole was shorter than the length between two sills. In the case of the present experiment, as the scour hole develops along the whole flume, the expressions proposed by Gaudio et al. (2000) can not be used.

Hoffmans and Pilarczyk (1993) carried out experiments devoted to a sill followed by a non-erodible horizontal bed located upstream of an erodible bed. The analysis of these experiments reveals four stages in the erosion process:

- Initiation of the erosion: the flow is not significantly perturbed by the creation of the scour hole. In the present experiment, this stage is very short.
- Development of the scour hole: the length and the depth of the hole increase, the bed profiles are auto-similar.
- Stabilisation: the erosion process is slower because it reaches an equilibrium.
- Equilibrium: no change in the bed profiles.

These different stages take place in the present experiments, but due to their too short duration the equilibrium stage is never reached. During the development stage, the authors proposed a simplified non-dimensional formulation

$$\frac{\left(z_b - z_0\right)_{\max}}{h_{w,0}} = \left(\frac{t}{t_0}\right)^{\beta} \tag{8.3}$$

where $h_{w,0}$ is the initial flow depth and t_0 is the time corresponding to a maximum scour depth equal to $h_{w,0}$. After analysing various data sets, Breusers (1967) deduced the coefficient β should be around 0.48.

Dargahi (2003), studying the scour hole downstream of a dissipative basin, also proposed a non-dimensional law for the evolution of the maximum scour depth with time

$$\frac{\left(z_b - z_0\right)_{\max}}{\left(z_b - z_0\right)_{\max,eq}} = \alpha\left(\frac{t}{t_{eq}}\right)^{\beta} \tag{8.4}$$

where $(z - z_0)_{\max,eq}$ is the maximum scour depth at the equilibrium stage, t_{eq} is the time corresponding to the equilibrium state and $\alpha \approx 1$.

The present experimental results agree with these non-dimensional formulations. In the case of run 7, the evolution of the maximum scour depth with time is plotted in Figure 8.6a, the interpolation curve is

$$\left(z_b - z_0\right)_{\max} = a\, t^{b} \tag{8.5}$$

where $a = 0.193$ and $b = 0.38$. It is presented in logarithmic scale in Figure 8.6b, the exponent b is the slope of the interpolation line. The interpolation is less accurate for the measurements corresponding to the end of the experiment. For times greater than 15000 s (approximately), the erosion process is in the stabilisation stage and no longer in the development stage corresponding to a non-dimensional formulation. If the measurements corresponding to times exceeding 15000 s are removed, the coefficients become $a = 0.164$ and $b = 0.4$. The exponent $b = 0.4$ is rather similar to the value of the exponent $\beta = 0.48$ (8.3) proposed by Breusers (1966). The coefficients a can not be compared to $h_{w,0} / t_0^{\beta}$ proposed by Hoffmans and Pilarczyk (1993) in (8.3) because in the present case, the maximum scour depth remains under the value of the initial water depth under the whole experiment. The equilibrium state is not reached at the end of the experiment, the erosion process is still in the stabilisation state in such a way that the coefficient a can not exactly be compared to $\alpha(z_b - z_0)_{\max,eq} / t_{eq}^{\beta}$ proposed by Dargahi (2003) (8.4). Nevertheless, if the last profile is considered as the equilibrium situation, one obtains $(z_b - z_0)_{eq} / t_{eq}^{\beta} = 0{,}143$, which is rather close to $a = 0{,}164$.

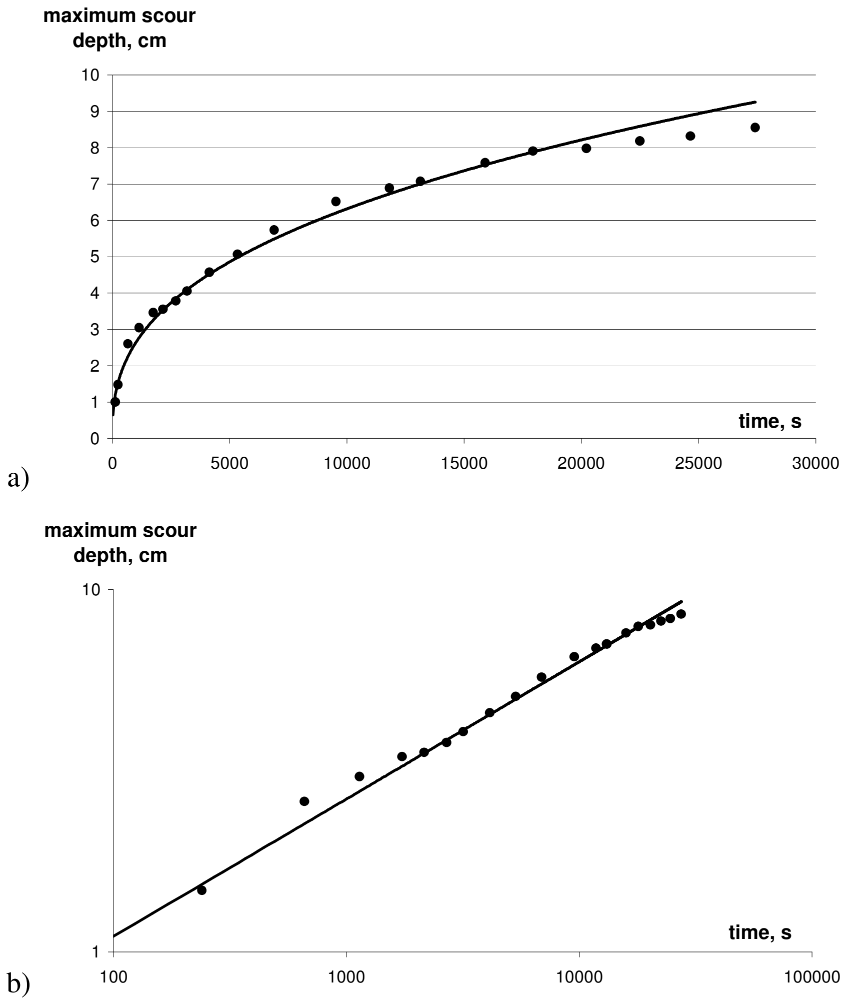

Figure 8.6. Maximum scour depth evolution:
(—) relation (8.5) with a = 0.193 and b = 0.38, (•) measurements

In order to model the evolution of the maximum scour through all the stages of the erosion process, Hoffmans and Pilarczyk (1993) proposed a more general non-dimensional exponential fit law

$$(z_b - z_0)^* = 1 - \exp\left(t^{*\gamma} \ln\left(1 - \frac{h_{w,0}}{(z_b - z_0)_{\max,eq}} \right)\right) \qquad (8.6)$$

where the non-dimensional parameters are

$$(z_b - z_0)^* = \frac{(z_b - z_0)_{\max}}{(z_b - z_0)_{\max,eq}} \quad \text{and} \quad t^* = \frac{t}{t_0} \tag{8.7}$$

and γ is a constant. As exposed before, this formulation is not directly applicable to the present case.

In the same way, Gaudio and Marion (2003), on the basis of an experimental work studying the erosion hole at the toe of a sill, proposed

$$(z_b - z_0)^* = 1 - \exp(-at^*) \tag{8.8}$$

where a is a constant and the definition of the dimensionless time t^* becomes

$$t^* = \frac{t}{t_s} \quad \text{where} \quad t_s = \frac{A_s}{q_s} \tag{8.9}$$

A_s is the scour area at the equilibrium state and q_s is the solid discharge at the beginning, before the scour hole creation. Using this relation, Gaudio and Marion (2003) were able to represent all their experiments on the same non-dimensional figure.

Assuming the equilibrium is reached, runs 4, 7 and 8 (the 3 longest experiment in Table 8.1) can be plotted on the same figure and can be compared to relation (8.8) (Fig. 8.7).

To check if the equilibrium state is reached, the experiments should have lasted longer. Nevertheless, the experimental measurements correspond to relation (8.8) with a = 1.5, which is quite different from a = 0.418 proposed by Gaudio and Marion (2003) for longer experiments with different parameter values.

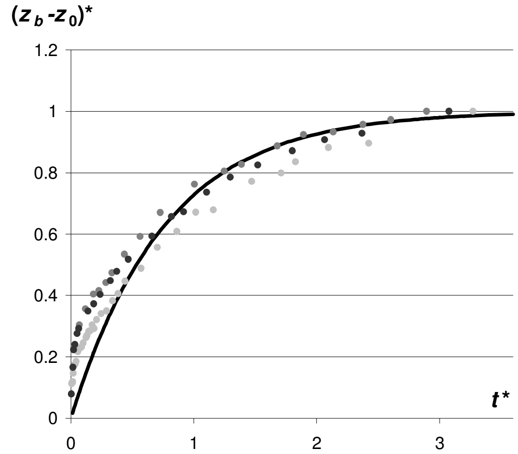

Figure 8.7. Non-dimensional maximum scour depth evolution : (━) relation(8.8) with a = 1.5, (•) measurements

8.2.2.3. Solid discharge

Using the approximate integration of the Exner equation (2.9) with a finite-difference method as proposed by Bell and Sutherland (1983), the solid discharge along the flume can be deduced from the variation of the bed level in time.

$$(1-\varepsilon_0)\frac{z_{b,x+\Delta x/2,t+\Delta t}-z_{b,x+\Delta x/2,t}}{\Delta t}=\frac{q_{s,x+\Delta x,t+\Delta t/2}-q_{s,x,t+\Delta t/2}}{\Delta x} \quad (8.10)$$

where space and time are discretised as illustrated in Figure 8.8. 5-cm space intervals Δx can be defined between each measurement point from the bed transition.

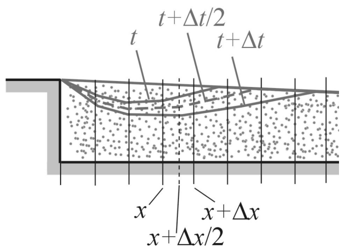

Figure 8.8. Discretisation in time and space to calculate the experimental solid discharge

The bed level $z_{b,x+\Delta x/2}$ at the middle of each interval can be deduced by interpolation of the bed level at the interval boundary $z_{b,x}$ and $z_{b,x+\Delta x}$. The variation of the bed level at the midpoint $(x + \Delta x/2)$ of the space interval Δx during a time Δt depends on the difference between the solid discharge (averaged on time) entering and exiting the concerned interval. Knowing that the solid discharge at the transition from fixed to erodible bed (upstream interface of the first interval) is equal to zero, it is possible to estimate the solid discharge along the flume (Fig. 8.9).

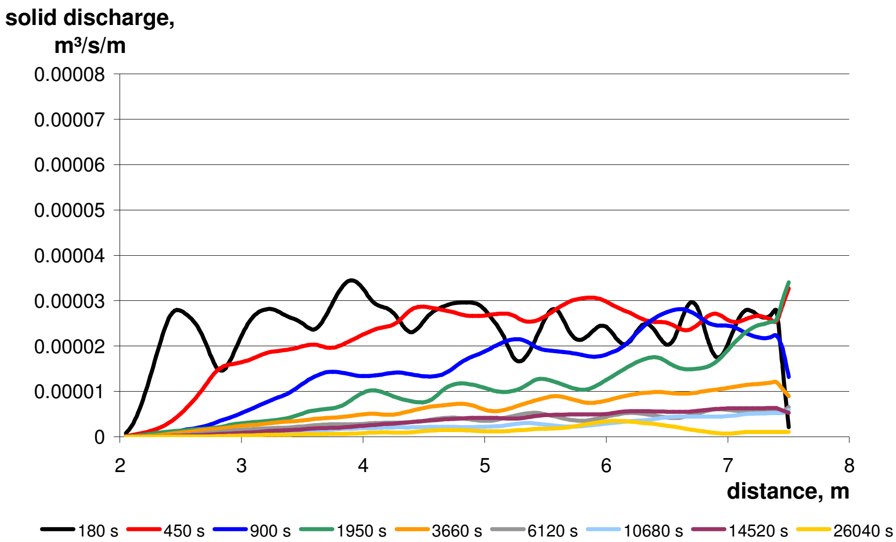

Figure 8.9. Evolution of the experimental solid discharge

The solid discharge under equilibrium conditions can be estimated from a common sediment transport formula like the one proposed by Meyer-Peter–Müller. The equilibrium solid discharge along the flume is plotted in Figure 8.10, which can be compared to Figure 8.9. The equilibrium solid discharge is quite irregular in space due to the presence of bed-forms. As the shear stress acting on the bed decreases with time, the solid discharge also decreases with time. Excepted at the end of the experiment, the equilibrium solid discharge calculated with the Meyer-Peter–Müller formulation overestimates the effective sediment transport rate. The main difference between the two discharges occurs in the first 50 cm downstream from the bed transition. In this zone, the equilibrium discharge decreases till it reaches a minimum value (corresponding to the maximum scour depth). At the opposite, the effective solid discharge increases from zero at the transition. Downstream of this area, both solid discharges follow the same evolution.

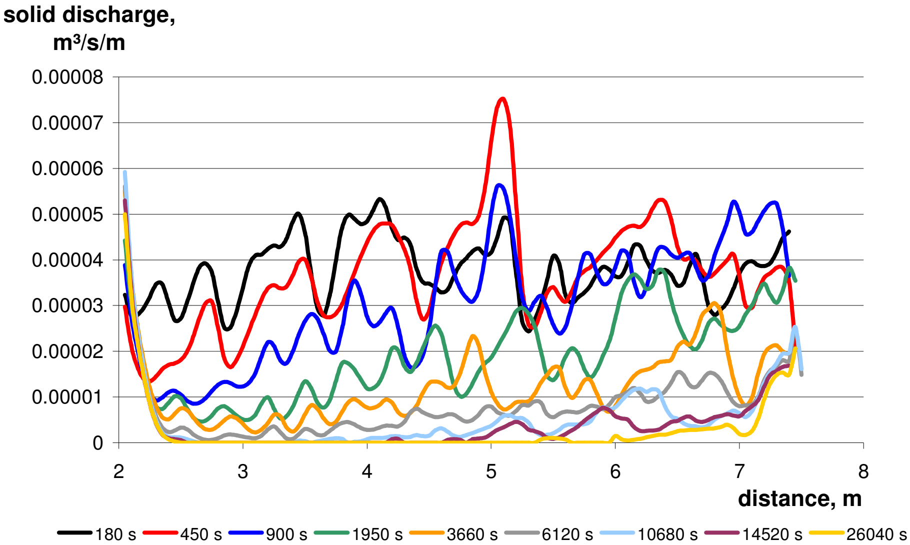

Figure 8.10. Evolution of the solid discharge: estimation with the Meyer-Peter–Müller formula

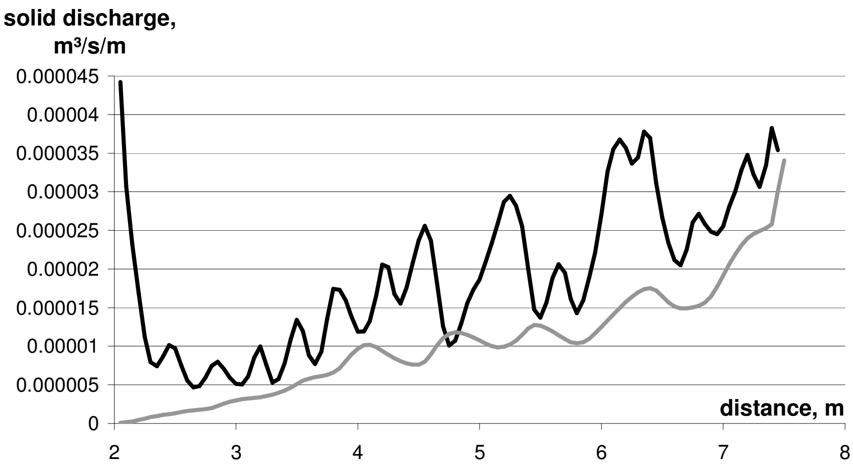

Figure 8.11. Solid discharge: experimental value (▬) and estimation with the Meyer-Peter–Müller formula (▬) for t = 1950 s

The equilibrium and the effective solid discharges are compared for t = 1950 s in Figure 8.11.

In order to determine a spatial lag for sediment transport, Bell and Sutherland (1983) defined the deficit depending on the ratio between the effective sediment transport q_s and the sediment transport under equilibrium conditions $q_{s,eq}$.

$$\Delta_s = 1 - \frac{q_s}{q_{s,eq}} \tag{8.11}$$

Based on their experimental measurements, the authors were able to establish a linear relation between the logarithm of the deficit and the distance from the transition.

$$\ln\left(\Delta_s(x,t)\right) = \alpha(t)\,x \quad \text{or} \quad \frac{q_s(x,t)}{q_{s,eq}(x,t)} = 1 - e^{-\alpha(t)x} \tag{8.12}$$

where the parameter α is varying with time. This law, available in the region of the scour hole, allows to calculate the effective solid discharge based on the equilibrium discharge. The deficit is plotted (logarithmic scale) as a function of the distance in the case of the present experiment for run 8 in Figure 8.12.

The deficit plotted in Figure 8.12 can be approximated by straight lines (with the deficit plotted using a logarithmic scale). It corresponds to expression (8.12), where the coefficient $\alpha(t)$ becomes less and less negative with time. The expression (8.12) was previously confirmed by the experiments of Bell and Sutherland (1992).

From the derivative of this expression, they deduced a spatial and temporal lag law.

$$\frac{\partial q_s}{\partial x} = \alpha(t)\left(q_{s,eq} - q_s\right) + \frac{q_s}{q_{s,eq}}\frac{\partial q_{s,eq}}{\partial x} \tag{8.13}$$

A simplified law was previously proposed by Daubert and Lebreton (1967) inspired by the work of Einstein (1950)

$$\frac{\partial q_s}{\partial x} = \alpha(t)\left(q_{s,eq} - q_s\right) \tag{8.14}$$

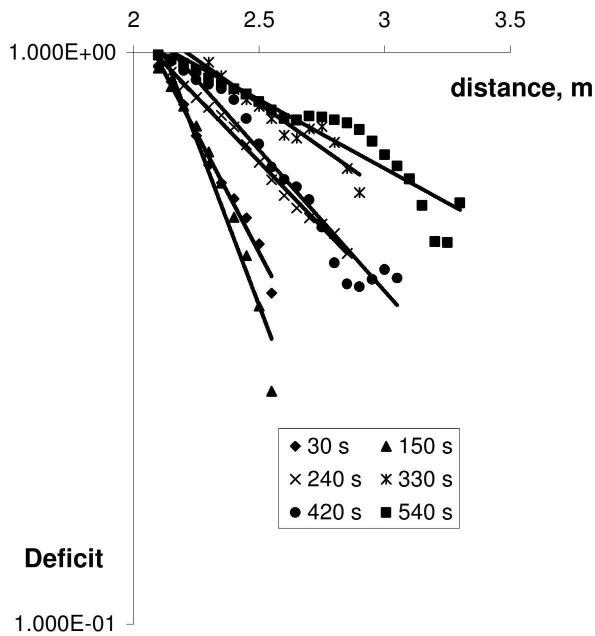

Figure 8.12. Deficit in logarithmic scale

8.2.3. Numerical modelling

The case of a flow over a transition between a non-erodible and an erodible bed is challenging for numerical modelling. It was interesting to test if the two-layer model is able to handle the solid discharge with spatial lag. The two-layer model, under different assumptions on the sediment concentration in the transport layer, is confronted to the classical approach of Saint-Venant–Exner.

The experiment modelled in this section is run 7 in Table 8.1. The non-erodible bed ($0 \leq x \leq 2$ m) is horizontal. Initially, the erodible bed ($S_0 = 0.0038$) is numerically approximated by a straight line and no sediment transport layer exists. The flow is modelled all along the flume. The upstream end of the numerical domain corresponds to the entrance of the flume.

There is no solid discharge introduced upstream and the bed is non-erodible at the entrance of the flume, then the flow is free of sediment at the upstream boundary. This implies that the two intermediate eigenvalues, related to sediments, are equal to zero and only the extreme characteristics, concerning hydrodynamics, remain. As the flow remains subcritical during the whole simulation, only one upstream boundary condition, concerning the liquid discharge $q_w = 0.077$ m³/s/m, has to be imposed. The downstream end corresponds to the downstream 2 cm-height weir. The flow upstream of the weir is subcritical, at the beginning, no sediment passes over the weir and a pure hydrodynamic control section is imposed. After a short time, sediments pass over the weir, there is a solid discharge at the outlet, three eigenvalues are positive and one is negative. The negative eigenvalue is fixed to zero in order to impose a mixed (water and sediment) control section at the downstream boundary. In the simulation, the sediment concentration in the transport layer is assumed to be identical to the one in the bed ($C_s = C_b = 0.57$). The friction coefficients ($C_{f,w} = 0.0115$ and $C_{f,s} = 0.39$) are calibrated on the basis of the experimental solid discharge (Fig. 8.9) and the Manning friction law.

The experimental and computed bed and water levels are compared in Figure 8.13. In general, the water level is well approximated by the numerical model. Concerning the computed bed level, even if the dunes are not reproduced, the part of the scour hole located downstream of the maximum scour depth is in good agreement with the experimental bed. Conversely, the upstream part of the scour hole (upstream of the maximum scour depth) calculated by the model is not similar to the experimental one. In the experiment, immediately downstream of the transition, there is a recirculating area where the velocity is lower. Then, the resulting shear stress acting on the bed and the erosion process are quite reduced. The two-layer model is not able to take into account this complex vertical velocity field because of the inherent uniform velocity profile assumption. As the velocity is averaged on the water depth, the bed shear stress and the erosion are overestimated in this region.

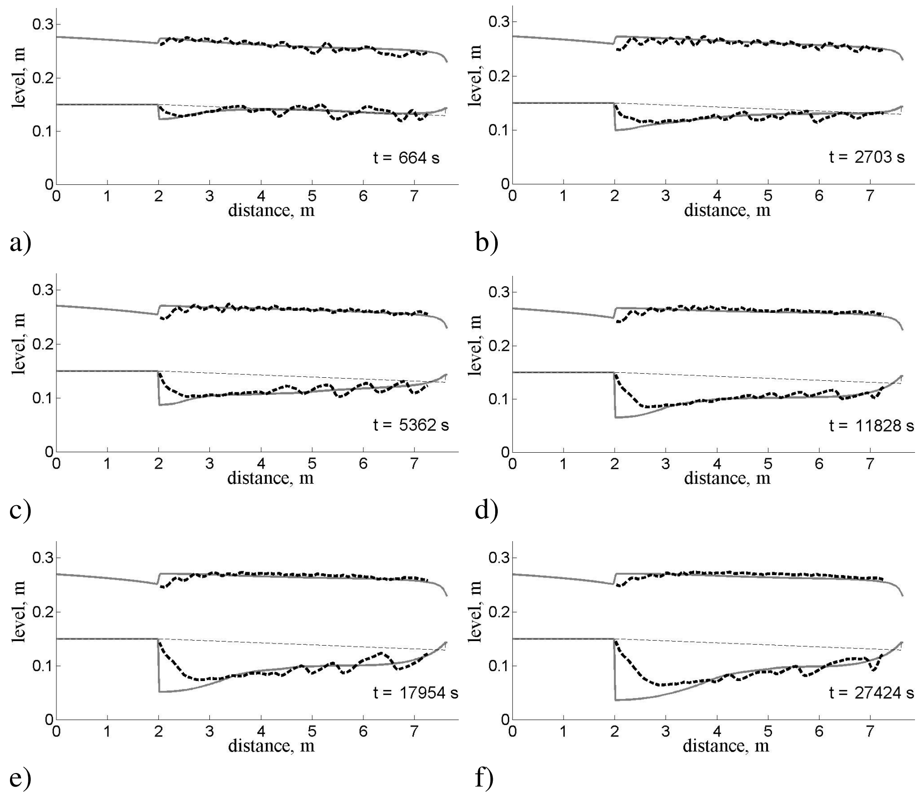

Figure 8.13. Comparison between experimental (▪▪▪▪) and computed (——)levels : time evolution (664 s – 27424 s) (initial bed (- - -))

The shape of the erosion hole could be artificially improved. If bed-slopes greater than the repose angle of the sediments were forbidden, the upstream part of the computed erosion hole would be artificially maintained at the repose angle. A more appropriate solution would be to treat the water in two separate layers in order to be able to take complex vertical velocity fields into account.

The computed solid discharge along the flume ($x > 2$ m) for several computational times is plotted in Figure 8.14.

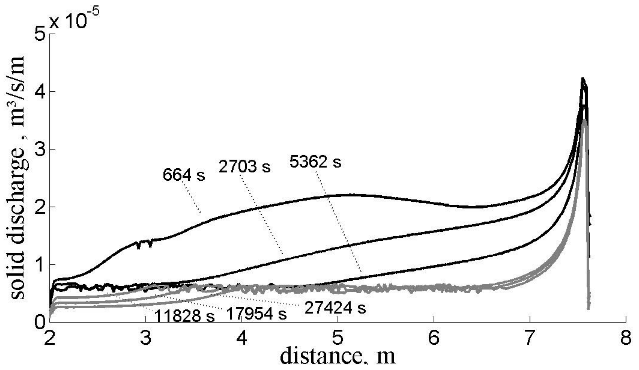

Figure 8.14. Evolution of the computed solid discharge q_s along the flume with time, first stage (▬) (t < 10000 s) and second stage (▬) (t > 10000 s)

Erosion and deposition depend on the variation of the solid discharge in space., At the bed transition, there is a sharp rise of the solid discharge, and then an important erosion, which develops in a short space (≈ 5 cm). Two stages can be identified in Figure 8.14. During the first part of the computation (t < 10000 s, black curves), downstream of the important erosion (at the transition), the solid discharge reaches a constant value, corresponding to an area without erosion or deposition. The size of this area increases with time. Downstream of this area, an erosion takes place till the weir is reached. Once the constant solid discharge area reaches the downstream weir (t ≈ 10000 s), the second stage begins (grey curves). The important erosion at the transition remains, but its amplitude decreases with time. It is followed by another erosion area (noticeable on the bed level in Figure 8.13d-f), which extends with time. During this second stage, the solid discharge at the downstream part of the channel does not change much with time. The computed solid discharge for $t = 1950$ s is compared to the experimental solid discharge deduced from Exner (8.10) and to the equilibrium solid discharge calculated with Meyer-Peter–Müller in Figure 8.15. The experimental and computed solid discharges have approximately the same variation with time, implying a quite good match between the experimental and computed bed levels. The two-layer model overestimates the solid discharge. It induces a difference at the transition, where the two-layer model calculates an erosion not existing in the experiment. Nevertheless, the solid discharge estimated by the two-layer model at the transition remains lower than the one calculated by Meyer-Peter–Müller.

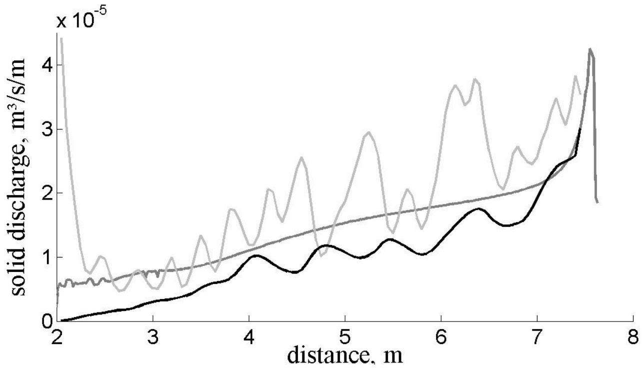

Figure 8.15. Solid discharge: experimental value (▬), computed with the two layer model (▬) and estimation with the Meyer-Peter–Müller formula (▬) for $t = 1950$ s

The time-evolution of the computed transport layer depth h_s along the flume is similar to the time-evolution of the computed solid discharge while the velocity ratio u_s / u_w is approximately constant (varying from 0.08 to 0.105). The velocity ratio is quite lower than for other test cases.

The eigenvalues for $t = 27424$ s are plotted in Figure 8.16. All are real, excepted at the downstream end where sediments pass over the weir. Three are positive and one is negative. In order to obtain a control section at the downstream end, the negative eigenvalue is set to zero there.

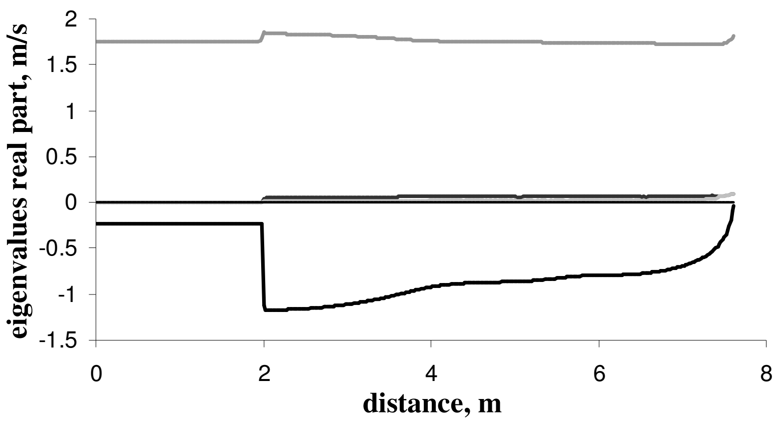

a)

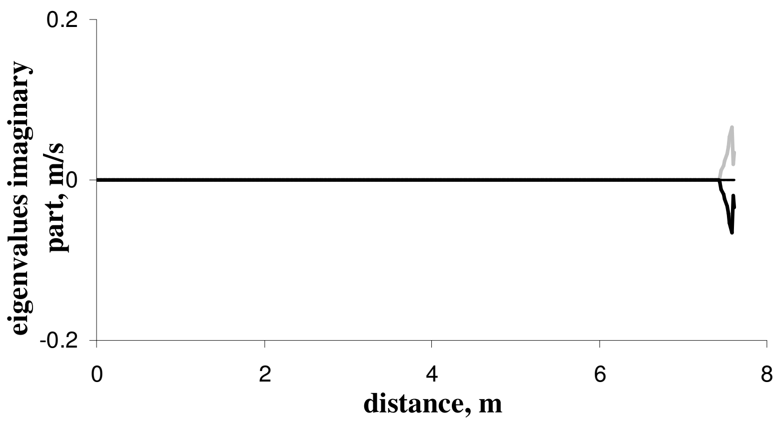

b)

Figure 8.16. Real (a) and imaginary (b) parts of the eigenvalues for $t = 27424$ s

8.2.3.1. Influence of the sediment concentration in the transport layer

The numerical results are greatly influenced by the value of the sediment concentration in the transport layer C_s. The results obtained when the concentration is assumed to be $C_s = 0.3$, which is lower than the concentration in the bed $C_b = 0.57$, are compared to the previous results in Figure 8.17. The friction coefficients ($C_{f,w} = 0.0115$ and $C_{f,s} = 0.528$) are calibrated on the same basis. At the beginning of the computation (Fig. 8.17a), the profiles are quite similar. For higher computational times ($t > 10000$ s) (Fig. 8.17b-c), in case of lower concentration $C_s = 0.3$ (grey curves), the erosion is lower at the transition, but more important at the middle of the channel. These differences are linked to a difference in the calculated solid discharges (Fig. 8.17d): even if the sediment discharge calculated by both models are quite close, on a long period, the slight differences in sediment discharge induce a significant dissimilarity in bed level. The maximum scour depth, contrarily to the bed level downstream, is more realistic when the concentration in the transport layer is smaller.

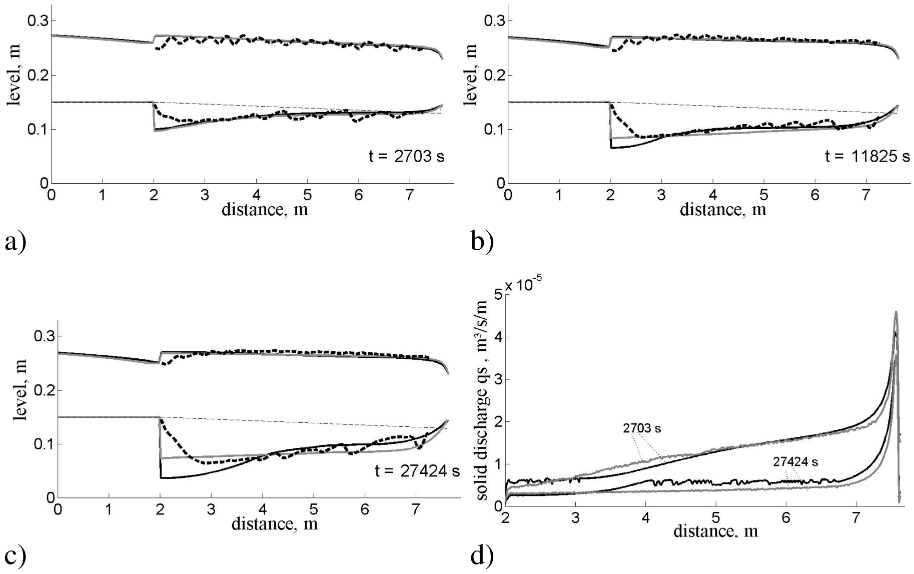

Figure **8**.17. Comparison between (a-c) experimental levels (▪▪▪▪) and the computed levels with $C_s = C_b = 0.57$ (▬) and with $C_s = 0.3$ (▬) (2703 s – 27424 s) (initial conditions (- - -)) (d) computed solid discharges

For initial conditions, there is no solid transport. The transport layer is created during the first computational steps. This creation process takes less than 1 s. The development of the transport layer during this process also depends on the assumption concerning the sediment concentration in the transport layer.

If the concentration in the bed and the transport layer are identical, the solid discharge rises till the end of the transport layer creation (Fig. 8.18). As the velocity in the transport layer u_s remains approximately constant during this stage, the transport layer depth h_s rises the same way as the solid discharge.

At the opposite, when the concentration in the transport layer is lower than in the bed, there is a overestimated rise of the solid discharge all along the flume at the beginning, then the solid discharge decreases till it reaches the value corresponding to flow conditions (Fig. 8.18). The overestimation of the solid discharge during the first time steps is due to overestimated transport layer depth h_s and velocity u_s.

In both cases, the solid discharge resulting from the creation process is the same, the time needed to reach this discharge, does not depend on the space and time discretisation.

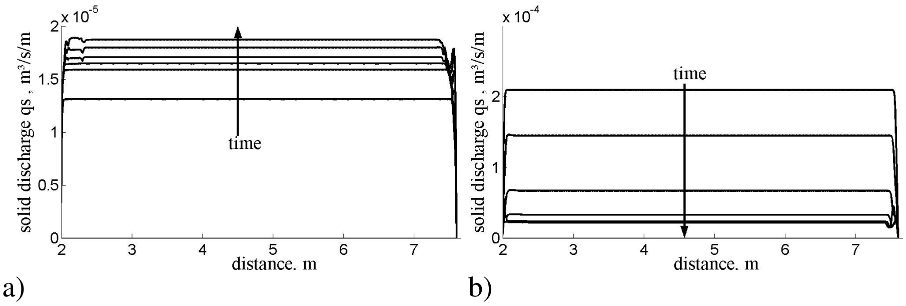

Figure 8.18. Creation of the transport layer (a) with $C_s = C_b = 0.57$ and (b) with $C_s = 0.3$

8.2.3.2. Comparison with Saint-Venant – Exner

The computation of the scour hole is made with the Saint-Venant – Exner model developed by Goutière and Laraichi (2006), the obtained numerical results are compared with the ones calculated by the two-layer model in Figure 8.19. A the beginning of the simulation (Fig. 8.19a-b), two different profiles are given for the Saint-Venant – Exner model, each corresponding to a different method to calculate the sediment discharge flux. The bed and water profiles in dark grey are the results from the simple sediment discharge flux expressed as the average of the sediment discharge in the neighbouring cells (7.4). As previously mentioned, this formulation of the flux induces instabilities due to the use of the Meyer-Peter–Müller formula, which is sensitive to small variations of the flow parameters. In the present case (Fig. 8.19a-b) oscillations are located in the downstream part of the flow, they are due to the sharp change in solid discharge at the transition between the erodible bed and the downstream weir (the sediment are stopped against the weir). Smaller perturbations are also located at the transition between the fixed and the mobile bed at the upstream boundary of the scour hole. For higher computational times, the profiles related to this flux formulation are not pictured anymore, because the instabilities, propagating along the whole channel, spoil the results. Then, as exposed in the case of the hydraulic jump (chapter 7 section 7.3.2.3), to smooth these discontinuities, a diffusive term is added in the expression of the sediment flux (7.7), the corresponding profiles are in light grey in Figure 8.19a-d. As the additional diffusive term takes into account the local and the equilibrium slopes, in the case of an adverse slope, the solid discharge flux calculated with this term is lower than if it was calculated without. It explains the slight difference between the bed levels calculated with both Saint-Venant – Exner methods in Figure 8.19a-b. It also explain the two low erosion illustrated in Figure 8.19d.

At the beginning of the experiment (Fig. 8.19a-b), the shape of the upstream part of the erosion hole is different for the two-layer and the Saint-Venant – Exner model. The bed profile obtained with Saint-Venant – Exner is tangential to the vertical in opposition with the one obtained with the two-layer approach, which is perpendicular. This variation is due to the difference in the solid discharge estimation. As previously underlined in Figure 8.15, both the two-layer model and the Meyer-Peter–Müller formula, used in the Saint-Venant – Exner model, overestimates the rise in solid discharge at the transition, inducing an excessive erosion. This overestimation of the solid discharge at the transition is even more significant for the Meyer-Peter-Formula.

The bed profile calculated with the Saint-Venant – Exner model in the final situation (Fig. 8.19d) does not correspond to reality, the erosion is underestimated upstream and overestimated downstream, partly due to the diffusive term, which tends to decrease the adverse slope.

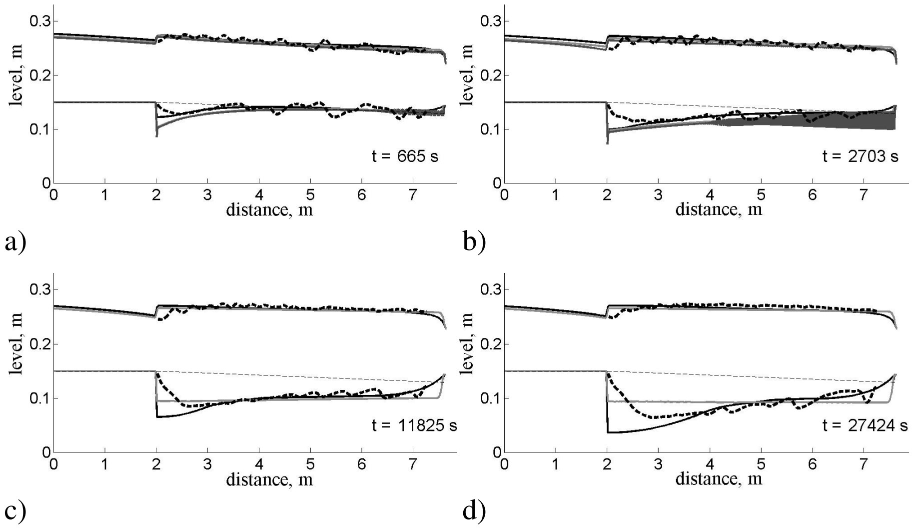

Figure 8.19. Comparison between experimental levels (▪▪▪▪) and the computed levels computed with the two-layer model $C_s = C_b = 0.57$ (▬) and with Saint-Venant – Exner with (▬) and without (▬) diffusion (665 s – 27424 s) (initial conditions (- - -))

8.3. Scouring at the toe of a sill

8.3.1. Experiment

In this section, the erosion occurring at the toe of a sill is studied. The idea of realising such an experiment comes from the case of the river Var, where several sills have been built (Rossi, 2002). Scour holes appeared at the toe of the sills inducing stability problems. Of course, this experiment, realised by Dewandre and Losseau (2004) for their Diploma work, is a very simplified and schematic version of the problem. The flow modelled includes instabilities linked both to transcritical flows and to the transition from a non-erodible to an erodible bed.

The experiments were carried out at the Civil Engineering Laboratory of the Université catholique de Louvain, using the experimental set up described in chapter 5. The upstream part of the flume is fitted with a non-erodible sill (Figs.8.20 and 8.21). At the toe of the non-erodible sill, there is a 13 cmthick layer of sand. The erodible bed at the toe of the sill is horizontal and the water level is imposed by a downstream weir, which is 2 cm above the downstream bed level.

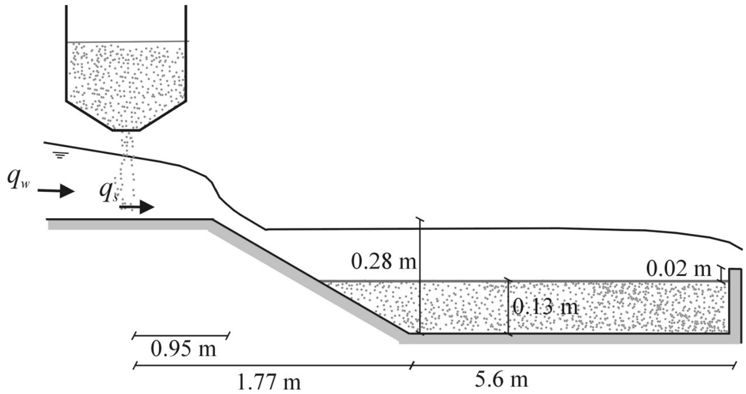

Figure 8.20. Experimental configuration

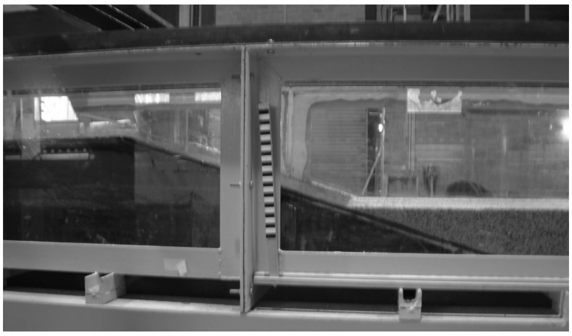

Figure 8.21. Picture of the sill

The bed and the water levels were measured simultaneously, respectively with the bed profiler and the ultrasonic probe described in chapter 5 section 5.5. Several experiments were performed within the ranges of water and sediment discharges reported in Table 8.2. In the experiments with an upstream sediment income, a slope of sediment equal to the equilibrium slope is pre-formed in the upstream part of the sill. It allows a sediment transport over the sill since the beginning of the experiment.

Run #	Q_w (l/s)	Q_s (l/s)	Duration (min)
Run 1	11	0	39
Run 2	9	0	48
Run3	9	0	227
Run 4	13	0	46
Run5	9	0.018	52
Run 6	9	0.018	48
Run 7	11	0.018	44
Run 8	11	0.018	130
Run 9	13	0.018	51
Run 10	13	0.0385	50
Run 11	11	0.0385	57
Run 12	9	0.0385	51
Run 13	13	0.0872	33
Run 14	16	0.0872	44

Table 8.2. Experimental data

In initial conditions, the bed is saturated with water by means of a small water discharge, and then, the water discharge is increased to its nominal value. The supercritical flow over the sill reaches the toe of the sill with a great velocity meaning an important erosion capacity. The sediments located at the toe of the sill are expelled and settle a little further, forming a bump (Fig. 8.22).

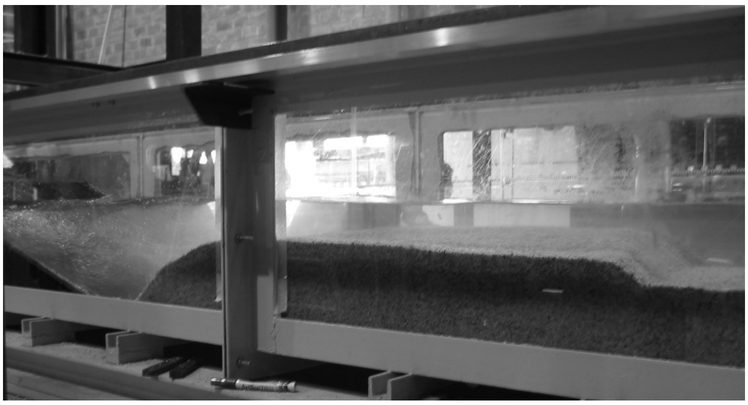

Figure 8.22. Scour hole, deposition and sediment front

The evolution of the scour hole depends on the sediment inflow : the lower the sediment income is, the more important the erosion will be. If the sediment inflow is too important, the erosion hole is quickly filled, and the sill becomes covered with sand. During the experiment, the bump located downstream of the scour hole slightly flattens, its downstream part is a front propagating downstream (Fig. 8.22). Its propagation is also depending on the sediment supply: the propagation is faster and the bump is less flattened when the sediment income is important. Over the bump, the flow is near critical and the resulting flow is unsteady. Sometimes, bed-forms (antidunes) are observed, otherwise, in critical condition, they are washed away. Figures 8.23 and 8.24 illustrate this evolution for run 3 (Table 8.2). In the present thesis, only run 3, without sediment supply will be treated.

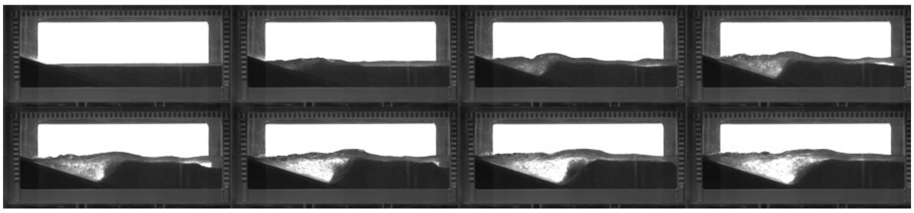

Figure 8.23. Evolution of the flow with time (time step = 10s)

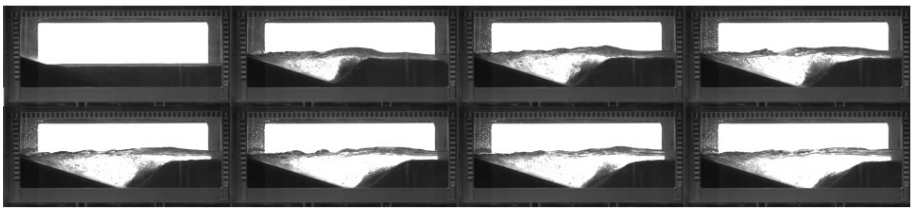

Figure 8.24. Evolution of the flow with time (time step = 60s)

Identically to the previous case of an erosion hole developing at the transition from fixed to erodible beds (Fig. 8.5), the self-similarity of the bed level in the scour area can be verified by plotting the bed level evolution on a non-dimensional way. Moreover, the maximum scour has the same kind of evolution (negative exponential) than the previous experiment (section 8.2.2.2), even if the empirical formulations are a little less appropriate. The supercritical flow, plunging in a flow characterised by a lower velocity can be assimilated to a water jet plunging into a pool. Hager (2004) realised an extensive experimental study on the latter case, giving non-dimensional formulae to calculate the maximum scour depth. There is a recirculating area in the scour hole, the flow is turbulent and the sand is in suspension (Fig. 8.25).

Figure 8.25. Recirculating area

8.3.2. Numerical modelling

The experiment modelled is run 3 in Table 8.2, the corresponding numerical domain is directly issued from the geometry described in Figure 8.20. The two-layer model assuming identical sediment concentration in the transport layer and in the bed ($C_s = C_b = 0.57$) is used. At the beginning of the experiment, the bed is saturated with a small water discharge ($q_w = 1$ l/s) to avoid sediment transport. Then, when the bed is saturated and the water level rises above the downstream weir, the water discharge is increased to its nominal value ($q_w = 9$ l/s). Obviously, in the experiment this change in discharge is rapid, but not instantaneous. The numerical initial conditions are simplified (Fig. 8.26a): a constant water depth ($h_w = 0.03$ m) and the small water discharge ($q_w = 1$ l/s) are imposed on the erodible bed, while the nominal water discharge ($q_w = 9$ l/s) and the corresponding water depth are imposed on the sill.

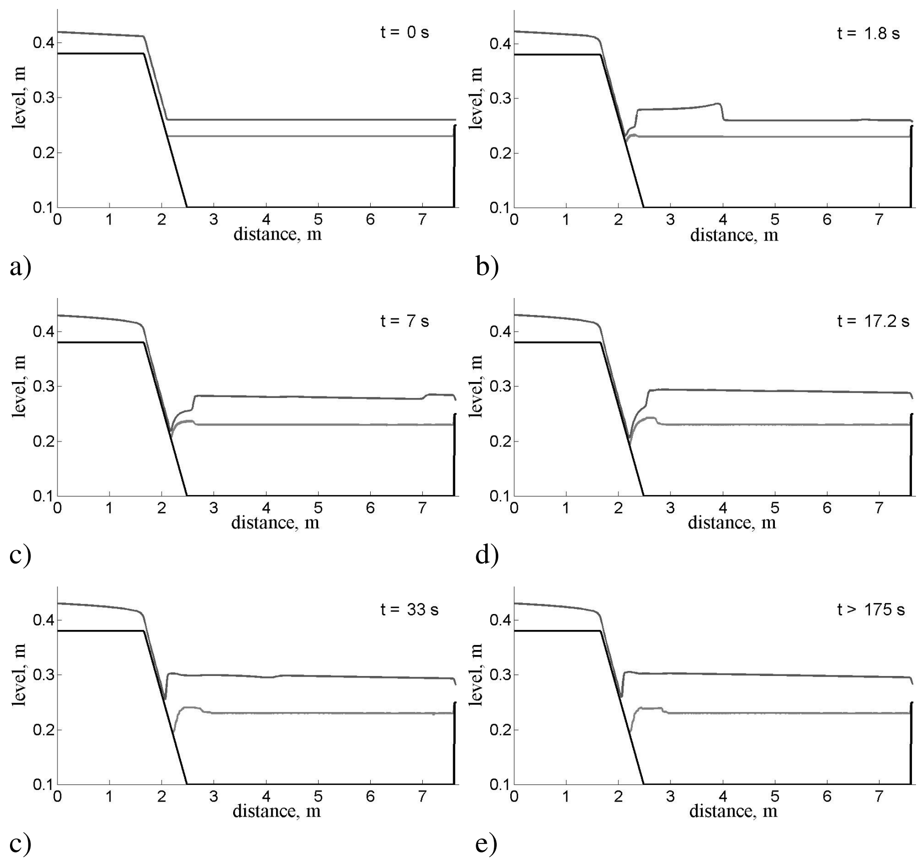

Figure 8.26. Computed levels: fixed bed (▬), bed and transport layer levels z_b and z_s (▬) and water level z_w (▬)

During the first computational times (Fig. 8.26), there is a fast adaptation of the water level. First, a water front propagates downstream (Fig. 8.26b). When the front arrives at the weir, it is reflected upstream (Fig. 8.26c). During this adaptation of the water level, the flow remains supercritical at the toe of the sill, inducing an erosion, the sediments eroded deposes downstream of the scour hole (Fig. 8.26b-d). The sediment front induced by the deposition and the hydraulic jump are located at the same place, the deposition area propagates downstream. As it is the case in the experiment, the scour hole at the toe of the sill follows the inclination of the sill. When the reflection coming from the downstream boundary reaches the hydraulic jump, the latter propagates upstream and becomes submerged against the sill

(Fig. 8.26e-f). During few seconds, the deposition area continues to propagate, then (8.26f) no sediment transport is observed anymore, and an equilibrium stage is reached.

In the experiment, the vertical velocity field at the submerged surge location is complex. Under the upper layer of water, which is a recirculating area where the velocity is low, the important velocity coming from the supercritical flow over the sill is still present, inducing erosion (Fig. 8.25). In accordance with the assumptions of the two-layer model, this complex velocity field cannot be reproduced. Indeed, in the two-layer model, the velocity profile in the water layer is assumed to be uniform on each vertical and the corresponding unique value of the velocity is the mean water velocity. At the submerged jump, the mean water velocity calculated by the model is lower than the velocity actually applied on the bed. Then, the shear stress applied to the bed in the model is underestimated, explaining why, once the surge becomes submerged, there is no sediment transport any more.

To be able to model such kind of flows, the model should be adapted in order to take into account a non-uniform repartition of the velocity on the depth. Perng (2006) modified the two-layer model in order to treat the parallel, but not identical, case of a water jet plunged in a basin in the direction of an erodible bed. The modified model is stratified as follows: (1) The water layer at rest which is assumed to be infinite; (2) the turbulent water layer, where the velocity is more important; (3) the transport layer, assuming this time suspension load and (4) the non mobile bed. The main changes in equations concern the source terms, new definitions have to be given to the shear stresses between the different layers. With some modifications allowing the first water layer to be finite with a specific velocity, the new model proposed by Perng (2006) should be more appropriate than the model described in this thesis.

The Saint-Venant – Exner model as described in this thesis is not able to reproduce such kind of flow. Karim and Ali (2001) modelled such kind of flow rather satisfactorily with the commercial model FLUENT, which contains several turbulent closure models.

8.4. Conclusions

Two experimental cases leading to the formation and the development of a scour hole were presented. Numerical models were confronted to both cases.

First, the scour hole occurring at the transition between a fixed and an erodible bed is modelled. As announced, the Saint-Venant – Exner model is not able to reproduce with satisfaction the erosion hole creation without appropriate spatial and temporal lags; nevertheless, qualitative results are obtained. Even if the profiles computed with the two-layer model are closer to the experimental ones in comparison with the Saint-Venant – Exner model, the results are not completely appropriate. Contrarily to other test cases, which were shorter in time, the assumption made on the sediment concentration in the transport layer has an important influence on the results. Even if the numerical sediment transport layer requires a little delay in space and time to develop, this delay seems shorter than the one observed in reality. Moreover, the shear stress applied to the bed at the transition is lower in the experiment than in the two-layer model, which does not take into account the recirculating area.

In the case of a scour hole at the toe of a sill, the velocity field is even more complex due to the presence of a submerged hydraulic jump. This time, the two-layer model underestimates the velocity and then the shear stress applied to the bed. The two-layer model, as formulated here, is not able to approach the experiment.

In both cases, in order to obtain results closer to reality at the transition, the model should be adapted to take complex vertical velocity distribution into account. The assumption of a uniform velocity distribution is not appropriate any more.